

Supplementary material for “Flexible Modelling of Time-Varying Exposures and Recurrent Events to Analyze Training Load Effects in Team Sports Injuries”

Lore Zumeta-Olaskoaga^{1,2}, Andreas Bender^{3,4}, and Dae-Jin Lee⁵

¹*BCAM - Basque Center for Applied Mathematics, Spain*

²*Departamento de Matemáticas, Universidad del País Vasco UPV/EHU, Spain*

³*Statistical Consulting Unit StABLab, Ludwig-Maximilians Universität München LMU, Germany*

⁴*Munich Center for Machine Learning (MCML), LMU München, Munich, Germany*

⁵*School of Science and Technology, IE University, Madrid, Spain*

In this document, we present the supplementary material that, to keep things brief, could not be included in our manuscript *Flexible Modelling of Time-Varying Exposures and Recurrent Events to Analyze Training Load Effects in Team Sports Injuries*. In Section A, we provide complementary analyses conducted on the football injury data; whereas in Section B, we give a more detailed explanation of the simulation study, outlining the data generation process and all the scenarios considered.

A Application: football injury data

A.1 Model specification and results

The log-hazard rate of player l of the model we fit is expressed as:

$$\log(\lambda(t|\mathbf{z}_l(t), b_l, i)) = \beta_0 + f_0(t_j) + z_l^{\text{type session}}(t_j)\beta_1 + g_1(\mathbf{z}_l^{\text{Speed}}, t) + g_2(\mathbf{z}_l^{\text{Dist}}, t) + b_l \quad (1)$$

$\forall t \in (\kappa_{j-1}, \kappa_j], \quad t_j := \kappa_j \text{ and } b_l \sim N(\mathbf{0}, \sigma_b),$

where:

- $\beta_0 + f_0(t_j)$ indicates the log-baseline hazard rate,
- $z_l^{\text{type session}}(t_j)$ the type of session undertaken by player l at t_j (whether match or training session),
- g_1 and g_2 are non-linear time-varying effects of the training load variables, i.e. the cumulative effects defined as, $\int_{\tau_{\text{Speed}}(t)} h(t-t_z) z_l^{\text{Speed}}(t_z) dt_z$ and $\int_{\tau_{\text{Dist}}(t)} h(t-t_z) z_l^{\text{Dist}}(t_z) dt_z$,
- and b_l a Gaussian random intercept term associated with player l .

The lag-lead windows are defined to be large enough to identify relevant past exposure effects by fitting a PAMM with a ridge penalization. In this regard, we define $\tau_{\text{Speed}}(t) = \tau_{\text{Dist}}(t) = \{t_z : t > t_z \wedge t < t_z + 11\}$, meaning that all *Speed* and *Dist* values recorded in the last 10 sessions prior to t (i.e. approximately three weeks before) can have an effect on the hazard of injury at time t .

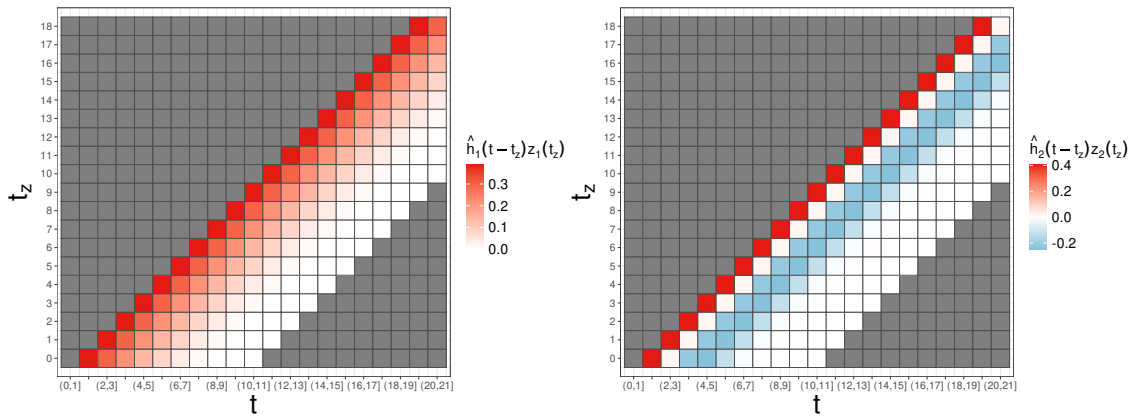


Figure S1: Estimated partial effects for covariates *Speed*, $\hat{h}_1(t - t_z)z_1(t_z)$, (left panel) and for *Dist*, $\hat{h}_2(t - t_z)z_2(t_z)$, (right panel) displayed over their respective lag-lead windows. Note: lag-lead windows are cut for the sake of clarity.

The estimated partial effects for different combinations of t and t_z , with $z^{\text{Speed}}(t_z) = 3.9 \forall t_z$ and $z^{\text{Dist}}(t_z) = 4700 \forall t_z$, and the resulting cumulative effects, $\hat{g}(z^{\text{Speed}}, t)$ and $\hat{g}(z^{\text{Dist}}, t)$, are shown in Figures S1 and S2, respectively. In Table S1 the summary of the estimated model coefficients is shown, and in Figure S3, the shapes of the estimated smooth baseline and player random effect are shown.

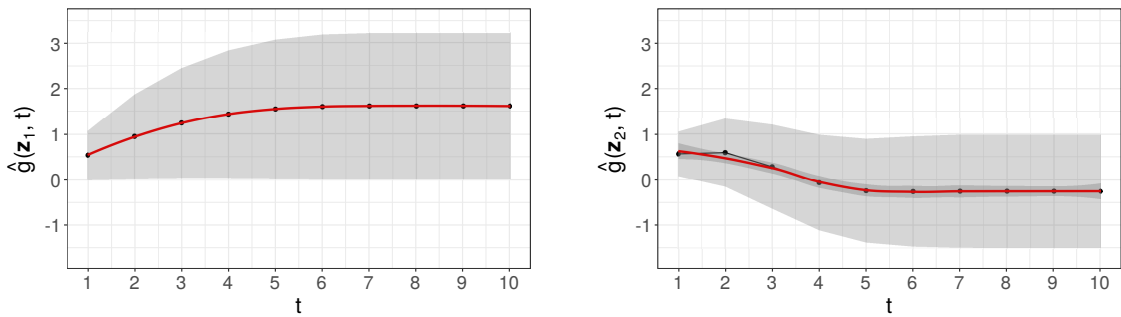


Figure S2: Estimated cumulative effects, $\hat{g}(z_1, t) = \hat{g}(z^{\text{Speed}}, t)$ and $\hat{g}(z_2, t) = \hat{g}(z^{\text{Dist}}, t)$, for $z^{\text{Speed}}(t_z) = 3.9 \forall t_z$ and $z^{\text{Dist}}(t_z) = 4700 \forall t_z$, respectively.

Table S1: Model summary

A. parametric coefficients	Estimate	Std. Error	t-value	p-value
(Intercept)	-7.2664	0.9198	-7.8997	< 0.0001
Type session:match	2.4481	0.2679	9.1371	< 0.0001
B. smooth terms	edf	Ref.df	F-value	p-value
Baseline	2.1280	2.6029	11.1358	0.0109
Speed cumulative effect	0.8981	1.1243	4.5324	0.0522
Dist cumulative effect	2.4947	2.9676	11.2029	0.0195
Player random effect	9.2944	35.0000	14.2589	0.0373

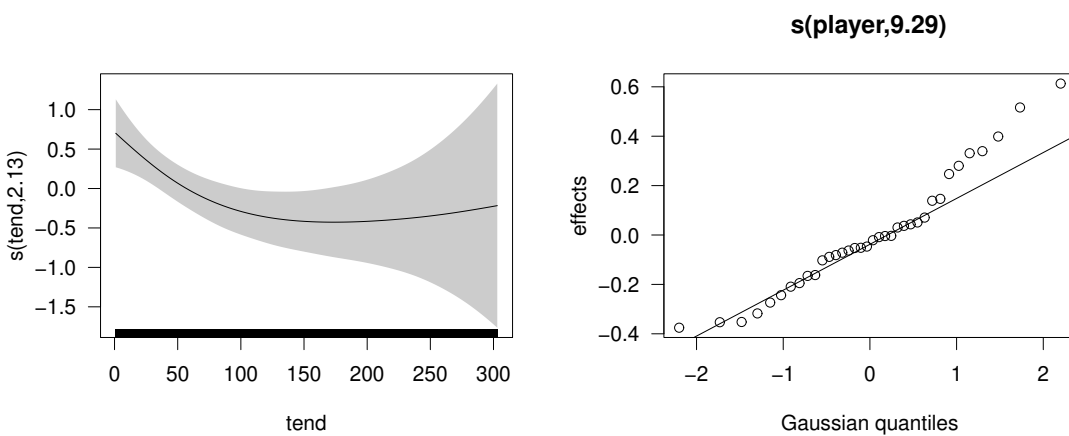


Figure S3: Estimated log-baseline hazard, the shaded area representing the point-wise 95% CI (left); and a quantile-quantile plot for the player random effect (right).

A.2 Comparison to conventional training load measures

We consider two measures widely used in the sports medicine and exercise physiology literature, namely, ACWR with rolling averages (RA) and ACWR with exponentially weighted moving averages (EWMA), as well as the unweighted sum of the past training exposures.

ACWR stands for acute chronic workload ratio and was introduced to model the relationship between changes in load and injury risk (Killen, 2010; Gabbett, 2016). It is a ratio describing the acute training load (e.g. the training load of the last week) to the chronic load (e.g. the training load of the last 4 weeks).

The concept is based on Banister's fitness-fatigue model (Banister, 1980) where the acute load dictates the "fatigue" state of an athlete, whereas the chronic load dictates the athlete's overall "fitness".

They are intended to reflect the athlete's preparedness. The ACWR measure compares the load the athlete has performed (acute) relative to the load the athlete has prepared for (chronic). The time frames (or windows) for acute and chronic workloads represent the time needed to dissipate the negative (fatigue) and positive (fitness) effects of training. In general terms:

$$\text{ACWR} := \frac{\text{Acute Load}}{\text{Chronic Load}}.$$

Commonly, and despite critiques, the rolling average (RA) has been the most frequently used method to account for the cumulative effects of acute and chronic training load. The rolling average of a training load variable denoted by z , over a n -sized time-lag window, at time t , is defined by:

$$\text{RA}_{n,t}(z) = \frac{z_{t-n+1} + z_{t-n+2} + \dots + z_t}{n}.$$

Alternatively, exponentially weighted moving averages (EWMA) have been proposed to summarize the cumulative effects of training load. In this case, EWMA at time t is defined as:

$$\text{EWMA}_t(z) = z_t \cdot \lambda_a + (1 - \lambda_a) \cdot \text{EWMA}_{t-1}(z),$$

with the time decay constant typically defined by $\lambda_a = \frac{2}{N+1}$, where N is 7 and 28 days, for acute and chronic loads, respectively. This measure acknowledges the weekly variations

in load. The effect of training decays over time since it places "more weight" on recent loads and less on distant ones in the past.

Then, one can compute ACWR using either rolling averages or EWMA to quantify the acute and chronic load. Typically, 7 and 28 days are used, respectively, as the time-lag windows of the acute (numerator) and chronic (denominator) training load.

These measures have been largely discussed and criticised in the literature, as they have several conceptual and mathematical limitations. We refer the reader to Wang (2020) for a thorough review and discussion.

In summary, the models we consider differ only in the definition of the cumulative effects:

- **ACWR (rolling avg.) model.** All the model terms of the main model remain the same except for the cumulative effects of z^{Speed} and z^{Dist} , which we replace with:

$$g(\mathbf{z}, t) = \text{ACWR}_t(\mathbf{z}) = \frac{\text{RA}_{7,t}(\mathbf{z})}{\text{RA}_{28,t}(\mathbf{z})}.$$

- **ACWR (EWMA) model.** All the model terms of the main model remain the same except for the cumulative effects of z^{Speed} and z^{Dist} , which we replace with:

$$g(\mathbf{z}, t) = \text{ACWR}_t(\mathbf{z}) = \frac{\text{EWMA}_{7,t}(\mathbf{z})}{\text{EWMA}_{28,t}(\mathbf{z})}.$$

- **Unweighted sum model.** All the model terms of the main model remain the same except for the cumulative effects of z^{Speed} and z^{Dist} , which we define as the cumulative (unweighted) sum of the past six exposures (sessions), i.e.:

$$g(\mathbf{z}^{\text{Speed}}, t) = \sum_{t_z < t}^{t_z > t-7} z^{\text{Speed}}(t_z) \text{ and } g(\mathbf{z}^{\text{Dist}}, t) = \sum_{t_z < t}^{t_z > t-7} z^{\text{Dist}}(t_z).$$

To compare the model performance, we compute likelihood-based measures. The results are shown in Table S2, ordered from the best performance to the least, according to the BIC measure.

Table S2: Likelihood-based measures regarding the goodness-of-fit of the fitted models, ordered from the best performance to the least, according to BIC

Model	AIC	Deviance	Deviance Explained	BIC
PAMM WCE ridge model	717.21	539.58	20.57	866.41
Unweighted sum model	802.74	628.49	7.48	924.92
ACWR (rolling avg.) model	804.24	625.67	7.89	950.49
ACWR (EWMA) model	796.74	616.54	9.24	951.02

B Simulation study

To evaluate the performance of the three models, that is, PAMMs with WCE-type cumulative effects: with no constraint (*Uncons.*), adding a constraint (*Constr.*) and adding a ridge penalty (*Ridge*); we simulate $N_{\text{sim}} = 500$ times a cohort of $L = 500$ individuals with exposures recorded at $t_{z,1} = 1, t_{z,2} = 2, \dots, t_{z,Q=40} = 40$ days before the time at which we model the hazard, $\mathbf{z}_l = (z_l(t_{z,1}), z_l(t_{z,2}), \dots, z_l(t_{z,Q}))$. Individuals' follow-up starts after 40 days of exposure, such that every individual has a complete exposure history of 40 exposures at the beginning of the follow-up.

In the following, we describe the scenario settings that were kept fixed across the simulation runs (section B.1), the data generation part that was random (section B.2) and the performance measures used to evaluate the results (section B.4). Finally, we present the simulation results we obtained (section B.5). The **R** code to reproduce these analyses is available at <https://github.com/lzumeta/flex-mod-training-loads-recu-injuries>.

B.1 Simulation scenarios

We set four different true weight functions for the WCE-type (i.e. partial effects of $h(t, t_z, z(t_z)) = h(t - t_z)z(t_z)$ type) cumulative effects, **(a)-(d)**, each defined over a $[0, Q]$ interval, and under three different levels of heterogeneity between recurrent events, $\sigma_b \in \{0.05, 0.5, 1\}$, indicating very low heterogeneity, low heterogeneity and high heterogeneity, respectively.

For the true weight functions of the WCE-type cumulative effect, we stand on and adapt the simulation setting presented in Sylvestre (2009) for cumulative effects of time-dependent exposures in Cox's PH model, and set the following six true weight functions:

- (a)** *Exponential decay:* $h(t - t_z) = \frac{4.5}{100}e^{-\frac{1}{10}(t-t_z)}$.
- (b)** *Bi-linear:* $h(t - t_z) = (1 - \frac{t-t_z}{25}) * 0.04$ for $t - t_z \leq 25$ and 0 otherwise.
- (c)** *Early peak:* probability density function of $N(0.04; 0.06)$ left-truncated at $t = 0$.
- (d)** *Inverted U:* probability density function of $N(0.2; 0.06)$ left-truncated at $t = 0$.

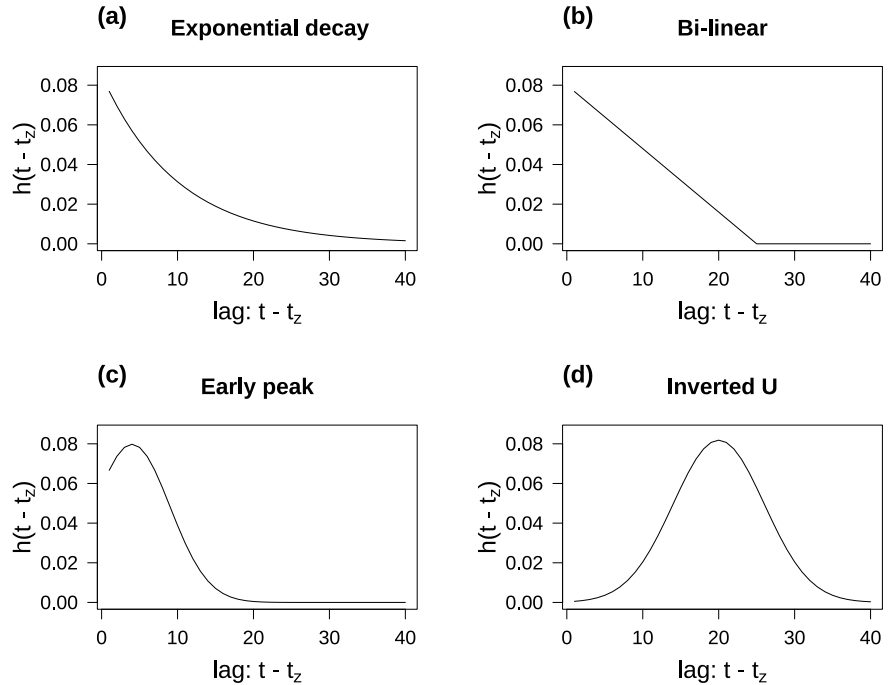


Figure S4: Each of the true weight functions, (a)-(d), considered.

Each function assigns weights to past exposures based on the time elapsed since the exposure occurred (see Figure S4). The first two functions, (a) and (b), assume that weights decrease monotonically as the time elapsed since exposure was recorded increases. Functions (c) and (d) are non-monotonic where the weights first increase and then decrease. In contrast to the function (d) (*inverted U*), in function (c) (*early peak*), the maximum weight is assigned to more recent exposures and from the 20-th lag on, the weights are zero. In other words, exposures recorded over 20 or more time units ago have no impact at the current time.

On the other hand, the number of events per subject, n_l , is kept fixed across all simulation runs. It is drawn from a truncated Poisson distribution with a lower truncation point equal to zero, so that we condition the variable, e.g. Y , to be $Y > 0$. The vector b_l associated with each individual l is drawn from a Gaussian distribution with a mean of 0 and a standard deviation $\sigma_b \in \{0.05, 0.5, 1\}$, and it is also kept fixed across all simulation runs and all true weight functions.

In this manner, we construct the underlying true hazard value, λ_{ij} ($l = 1, \dots, L = 500$, $i_l = 1, \dots, n_l$ and $j = 1, \dots, J = 40$), for each event of each subject (i_l) at each time

point (κ_j) . This value defines the intervals of the piece-wise constant hazard vector and remains fixed in each scenario of the simulation study. Each subject's hazard value can be seen as the sum of: an intercept, a smooth baseline, the cumulative effect and the random effect.

B.2 Generation of recurrent survival times

Once we have the vector of piece-wise constant hazards $\lambda = (\lambda_1, \lambda_2, \dots, \lambda_{J=40})$ in intervals defined by time points $\kappa = (\kappa_0, \dots, \kappa_{J=40})$, we replicate the rows of the data depending on the number of events that each individual is at risk of (we kept this number, i.e. n_l , fixed), in order to generate recurrent survival times. Then, we draw survival times from the piece-wise exponential distribution, i.e. $t \sim \text{PEXP}(\lambda, \kappa)$ for which the algorithm is summarized in Table S3. The main function to draw piece-wise constant rates is implemented in **R** as `msm::rpexp()`.

Table S3: Pseudo-algorithm for drawing survival times from the piece-wise exponential distribution (PEXP), adapted from Bender (2019)

Let κ_{j-1} be the left border of interval $(\kappa_{j-1}, \kappa_j]$, $j = 1, \dots, J$:

1. For $l = 1, \dots, L$:

 1.1. For $i_l = 1, \dots, n_l$:

 (a) Set $j = 1$

 (b) For $j = 1, \dots, J$

 i. Draw survival time $t'_{i_l j}$ from $\text{Exp}(\lambda_{i_l j})$, set $t_{i_l} = \kappa_{j-1} + t'_{i_l j}$

 ii. If $\kappa_{j-1} < t_{i_l} \leq \kappa_j$ or $j = J$: accept t_{i_l}

 iii. Else: $j = j + 1$

 1.2. Return vector of survival times (t_1, \dots, t_{n_l}) for subject l .

 1.3. Order the above survival times vector and the subject's i_l -th event number indicator (`enum`).

2. Return vector of survival times:

$(t_{11}, t_{21}, \dots, t_{n_1}, t_{12}, t_{22}, \dots, t_{n_2}, \dots, t_{1L}, t_{2L}, \dots, t_{n_L})$.

B.3 Model fitting

For model fitting, we use P-splines with second-order difference penalties and, 10 knots for the smooth baseline hazard term and 15 knots for the WCE-type smooth term. We use the restricted maximum likelihood (REML) optimization routine within the `mgcv` R package.

B.4 Performance measures

The performance measures we use to assess the performance of the models are the mean RMSE, mean 95% pointwise coverage, squared error, BIC and the deviance explained.

- The mean RMSE integrates the bias and the variance of \hat{h} into one summary measure. The root of the sum of squared differences between the estimated \hat{h} value and the true h value, computed across all covariates z and $t - t_z$ lag points, and then averaged over all the simulation runs.

$$\overline{\text{RMSE}}(h) = \frac{1}{N_{\text{sim}}} \sum_{n=1}^{N_{\text{sim}}} \sqrt{\frac{1}{N_{t_z}} \sum_{t-t_z=0}^{40} \left(h(t - t_z) - \hat{h}(t - t_z)^{(n)} \right)^2},$$

where $N_{t_z} = 41$, since $t - t_z = \{0, 1, 2, \dots, 40\}$ takes 40 +1 number of different values.

$$\text{RMSE}(\sigma_b) = \sqrt{\frac{1}{N_{\text{sim}}} \sum_{n=1}^{N_{\text{sim}}} \left(\sigma_b - \hat{\sigma}_b^{(n)} \right)^2},$$

- The mean 95% coverage measures the proportion that the estimated pointwise 95% confidence interval contains h . It is calculated as:

$$\overline{\text{Coverage}}_\alpha = \frac{1}{N_{\text{sim}}} \sum_{n=1}^{N_{\text{sim}}} \left[\frac{1}{N_{t_z}} \sum_{t-t_z=0}^{40} \mathbb{I} \left(h(t - t_z) \in \left[\hat{h}(t - t_z)^{(n)} \mp \zeta_{1-\alpha/2} \hat{\sigma}_{\hat{h}}^{(n)} \right] \right) \right],$$

where ζ_q is the q-quantile of the standard normal distribution and $\hat{\sigma}_{\hat{h}}$ the standard error of the estimated $\hat{h}(t - t_z)$. The closer to 0.95 the better.

- The squared error of σ_b is the summand of $\text{RMSE}(\sigma_b)$, i.e. $(\sigma_b - \hat{\sigma}_b)^2$.
- The BIC and Deviance Explained are likelihood-based measures formulated to assess the model's goodness of fit. As described in `?mgcv::gamObject`, $\text{BIC} = k \ln(n) - 2 \ln(\mathcal{L}(\text{model}|\text{data}))$ and $\text{deviance explained} = (1 - \text{residual deviance}/\text{null deviance})$. A smaller BIC indicates better performance, while a higher Deviance Explained suggests a better fit.

B.5 Simulation results

Next, we present the simulation study results:

- Tables S4-S7 present summary statistics for mean RMSE and mean Coverage $_{\alpha}$ of the estimated $h(t, t_z, z(t_z))$ and σ_b across all simulation settings.
- Figures S5-S7 show boxplots of the distribution of the RMSE of $h(t, t_z, z(t_z))$, the distribution of 95% point-wise coverage of $h(t, t_z, z(t_z))$ and the squared error of σ_b across all simulation settings.
- Figures S8-S19 display the estimated weight functions for each model across all simulation settings, with the true weight function represented by the thick black curve and the mean of the estimated curves depicted by the thick coloured curve.
- Table S8-S10 displays the proportion of times each model is considered the “best”, determined by either BIC or Deviance Explained in each simulation run across all settings. This represents the number of times a specific model has the lowest BIC or the greatest Deviance Explained among the three candidate models.

Table S4: Simulation results for $N_{\text{sim}} = 500$ in each scenario setting in terms of mean RMSE and mean coverage ($\alpha = 0.05$) of $h_{t,t_z,z(t_z)}$ and RMSE of σ_b

Data generation mechanism			Model	Mean RMSE	Mean Coverage	
WCE shape	L players	Heterogeneity		$h_{t,t_z,z(t_z)}$	σ_b	$h_{t,t_z,z(t_z)}$
(a) Exponential decay	L = 20	$\sigma_b = 0.05$	<i>Uncons.</i>	0.040	0.671	0.933
		$\sigma_b = 0.05$	<i>Constr.</i>	0.032	0.636	0.903
		$\sigma_b = 0.05$	<i>Ridge</i>	0.028	0.576	0.482
		$\sigma_b = 0.5$	<i>Uncons.</i>	0.041	0.580	0.917
		$\sigma_b = 0.5$	<i>Constr.</i>	0.033	0.551	0.882
		$\sigma_b = 0.5$	<i>Ridge</i>	0.027	0.501	0.534
	L = 40	$\sigma_b = 1$	<i>Uncons.</i>	0.042	0.683	0.916
		$\sigma_b = 1$	<i>Constr.</i>	0.034	0.634	0.888
		$\sigma_b = 1$	<i>Ridge</i>	0.028	0.603	0.591
		$\sigma_b = 0.05$	<i>Uncons.</i>	0.023	0.307	0.928
		$\sigma_b = 0.05$	<i>Constr.</i>	0.019	0.301	0.874
		$\sigma_b = 0.05$	<i>Ridge</i>	0.017	0.289	0.715
	L = 100	$\sigma_b = 0.5$	<i>Uncons.</i>	0.024	0.325	0.917
		$\sigma_b = 0.5$	<i>Constr.</i>	0.020	0.315	0.855
		$\sigma_b = 0.5$	<i>Ridge</i>	0.018	0.316	0.695
		$\sigma_b = 1$	<i>Uncons.</i>	0.023	0.365	0.933
		$\sigma_b = 1$	<i>Constr.</i>	0.019	0.349	0.888
		$\sigma_b = 1$	<i>Ridge</i>	0.017	0.356	0.700
		$\sigma_b = 0.05$	<i>Uncons.</i>	0.015	0.213	0.909
		$\sigma_b = 0.05$	<i>Constr.</i>	0.013	0.210	0.805
		$\sigma_b = 0.05$	<i>Ridge</i>	0.011	0.205	0.764
		$\sigma_b = 0.5$	<i>Uncons.</i>	0.015	0.211	0.916
		$\sigma_b = 0.5$	<i>Constr.</i>	0.013	0.213	0.804
		$\sigma_b = 0.5$	<i>Ridge</i>	0.012	0.215	0.777
		$\sigma_b = 1$	<i>Uncons.</i>	0.015	0.262	0.936
		$\sigma_b = 1$	<i>Constr.</i>	0.013	0.266	0.847
		$\sigma_b = 1$	<i>Ridge</i>	0.011	0.271	0.781

Table S5: Simulation results for $N_{\text{sim}} = 500$ in each scenario setting in terms of mean RMSE and mean coverage ($\alpha = 0.05$) of $h_{t,t_z,z(t_z)}$ and RMSE of σ_b (continuation)

Data generation mechanism			Model	Mean RMSE	Mean Coverage	
WCE shape	L players	Heterogeneity		$h_{t,t_z,z(t_z)}$	σ_b	$h_{t,t_z,z(t_z)}$
(b) Bi-linear	L = 20	$\sigma_b = 0.05$	<i>Uncons.</i>	0.040	0.655	0.936
		$\sigma_b = 0.05$	<i>Constr.</i>	0.032	0.622	0.897
		$\sigma_b = 0.05$	<i>Ridge</i>	0.028	0.577	0.771
		$\sigma_b = 0.5$	<i>Uncons.</i>	0.039	0.595	0.933
		$\sigma_b = 0.5$	<i>Constr.</i>	0.031	0.571	0.890
		$\sigma_b = 0.5$	<i>Ridge</i>	0.027	0.527	0.778
	L = 40	$\sigma_b = 1$	<i>Uncons.</i>	0.042	0.678	0.917
		$\sigma_b = 1$	<i>Constr.</i>	0.033	0.640	0.889
		$\sigma_b = 1$	<i>Ridge</i>	0.027	0.605	0.802
		$\sigma_b = 0.05$	<i>Uncons.</i>	0.023	0.309	0.926
		$\sigma_b = 0.05$	<i>Constr.</i>	0.019	0.311	0.818
		$\sigma_b = 0.05$	<i>Ridge</i>	0.016	0.300	0.901
	L = 100	$\sigma_b = 0.5$	<i>Uncons.</i>	0.023	0.324	0.925
		$\sigma_b = 0.5$	<i>Constr.</i>	0.019	0.308	0.815
		$\sigma_b = 0.5$	<i>Ridge</i>	0.017	0.306	0.882
		$\sigma_b = 1$	<i>Uncons.</i>	0.024	0.391	0.923
		$\sigma_b = 1$	<i>Constr.</i>	0.020	0.378	0.819
		$\sigma_b = 1$	<i>Ridge</i>	0.017	0.381	0.887
		$\sigma_b = 0.05$	<i>Uncons.</i>	0.015	0.199	0.920
		$\sigma_b = 0.05$	<i>Constr.</i>	0.013	0.196	0.778
		$\sigma_b = 0.05$	<i>Ridge</i>	0.011	0.191	0.908
		$\sigma_b = 0.5$	<i>Uncons.</i>	0.014	0.202	0.930
		$\sigma_b = 0.5$	<i>Constr.</i>	0.013	0.202	0.796
		$\sigma_b = 0.5$	<i>Ridge</i>	0.010	0.205	0.919
		$\sigma_b = 1$	<i>Uncons.</i>	0.014	0.252	0.945
		$\sigma_b = 1$	<i>Constr.</i>	0.013	0.255	0.816
		$\sigma_b = 1$	<i>Ridge</i>	0.010	0.260	0.932

Table S6: Simulation results for $N_{\text{sim}} = 500$ in each scenario setting in terms of mean RMSE and mean coverage ($\alpha = 0.05$) of $h_{t,t_z,z(t_z)}$ and RMSE of σ_b (continuation)

Data generation mechanism			Model	Mean RMSE	Mean Coverage	
WCE shape	L players	Heterogeneity		$h_{t,t_z,z(t_z)}$	σ_b	$h_{t,t_z,z(t_z)}$
(c) Early peak	L = 20	$\sigma_b = 0.05$	<i>Uncons.</i>	0.040	0.661	0.925
		$\sigma_b = 0.05$	<i>Constr.</i>	0.033	0.628	0.867
		$\sigma_b = 0.05$	<i>Ridge</i>	0.031	0.575	0.759
		$\sigma_b = 0.5$	<i>Uncons.</i>	0.040	0.574	0.916
		$\sigma_b = 0.5$	<i>Constr.</i>	0.034	0.558	0.861
		$\sigma_b = 0.5$	<i>Ridge</i>	0.030	0.516	0.787
	L = 40	$\sigma_b = 1$	<i>Uncons.</i>	0.041	0.572	0.918
		$\sigma_b = 1$	<i>Constr.</i>	0.034	0.558	0.871
		$\sigma_b = 1$	<i>Ridge</i>	0.030	0.533	0.809
		$\sigma_b = 0.05$	<i>Uncons.</i>	0.025	0.279	0.883
		$\sigma_b = 0.05$	<i>Constr.</i>	0.022	0.279	0.786
		$\sigma_b = 0.05$	<i>Ridge</i>	0.021	0.271	0.853
	L = 100	$\sigma_b = 0.5$	<i>Uncons.</i>	0.025	0.307	0.889
		$\sigma_b = 0.5$	<i>Constr.</i>	0.022	0.297	0.795
		$\sigma_b = 0.5$	<i>Ridge</i>	0.021	0.297	0.852
		$\sigma_b = 1$	<i>Uncons.</i>	0.025	0.385	0.915
		$\sigma_b = 1$	<i>Constr.</i>	0.021	0.372	0.845
		$\sigma_b = 1$	<i>Ridge</i>	0.020	0.375	0.879
		$\sigma_b = 0.05$	<i>Uncons.</i>	0.017	0.186	0.862
		$\sigma_b = 0.05$	<i>Constr.</i>	0.016	0.184	0.786
		$\sigma_b = 0.05$	<i>Ridge</i>	0.015	0.180	0.849
		$\sigma_b = 0.5$	<i>Uncons.</i>	0.017	0.209	0.884
		$\sigma_b = 0.5$	<i>Constr.</i>	0.016	0.211	0.794
		$\sigma_b = 0.5$	<i>Ridge</i>	0.015	0.215	0.869
		$\sigma_b = 1$	<i>Uncons.</i>	0.018	0.275	0.899
		$\sigma_b = 1$	<i>Constr.</i>	0.016	0.278	0.818
		$\sigma_b = 1$	<i>Ridge</i>	0.015	0.283	0.887

Table S7: Simulation results for $N_{\text{sim}} = 500$ in each scenario setting in terms of mean RMSE and mean coverage ($\alpha = 0.05$) of $h_{t,t_z,z(t_z)}$ and RMSE of σ_b (continuation)

Data generation mechanism			Model	Mean RMSE	Mean Coverage	
WCE shape	L players	Heterogeneity		$h_{t,t_z,z(t_z)}$	σ_b	$h_{t,t_z,z(t_z)}$
(d) Inverted U	L = 20	$\sigma_b = 0.05$	<i>Uncons.</i>	0.054	0.833	0.888
		$\sigma_b = 0.05$	<i>Constr.</i>	0.045	0.715	0.834
		$\sigma_b = 0.05$	<i>Ridge</i>	0.043	0.650	0.384
		$\sigma_b = 0.5$	<i>Uncons.</i>	0.050	0.691	0.875
		$\sigma_b = 0.5$	<i>Constr.</i>	0.043	0.647	0.822
		$\sigma_b = 0.5$	<i>Ridge</i>	0.043	0.600	0.377
	L = 40	$\sigma_b = 1$	<i>Uncons.</i>	0.051	0.787	0.883
		$\sigma_b = 1$	<i>Constr.</i>	0.044	0.708	0.827
		$\sigma_b = 1$	<i>Ridge</i>	0.043	0.670	0.409
		$\sigma_b = 0.05$	<i>Uncons.</i>	0.033	0.350	0.853
		$\sigma_b = 0.05$	<i>Constr.</i>	0.030	0.344	0.786
		$\sigma_b = 0.05$	<i>Ridge</i>	0.033	0.328	0.627
	L = 100	$\sigma_b = 0.5$	<i>Uncons.</i>	0.032	0.351	0.866
		$\sigma_b = 0.5$	<i>Constr.</i>	0.030	0.339	0.788
		$\sigma_b = 0.5$	<i>Ridge</i>	0.033	0.341	0.600
		$\sigma_b = 1$	<i>Uncons.</i>	0.032	0.366	0.870
		$\sigma_b = 1$	<i>Constr.</i>	0.029	0.352	0.794
		$\sigma_b = 1$	<i>Ridge</i>	0.033	0.357	0.605
		$\sigma_b = 0.05$	<i>Uncons.</i>	0.022	0.240	0.884
		$\sigma_b = 0.05$	<i>Constr.</i>	0.020	0.236	0.849
		$\sigma_b = 0.05$	<i>Ridge</i>	0.020	0.230	0.796
		$\sigma_b = 0.5$	<i>Uncons.</i>	0.021	0.232	0.876
		$\sigma_b = 0.5$	<i>Constr.</i>	0.020	0.233	0.836
		$\sigma_b = 0.5$	<i>Ridge</i>	0.020	0.235	0.795
		$\sigma_b = 1$	<i>Uncons.</i>	0.021	0.260	0.898
		$\sigma_b = 1$	<i>Constr.</i>	0.020	0.261	0.854
		$\sigma_b = 1$	<i>Ridge</i>	0.020	0.265	0.807

$L = 20$ players

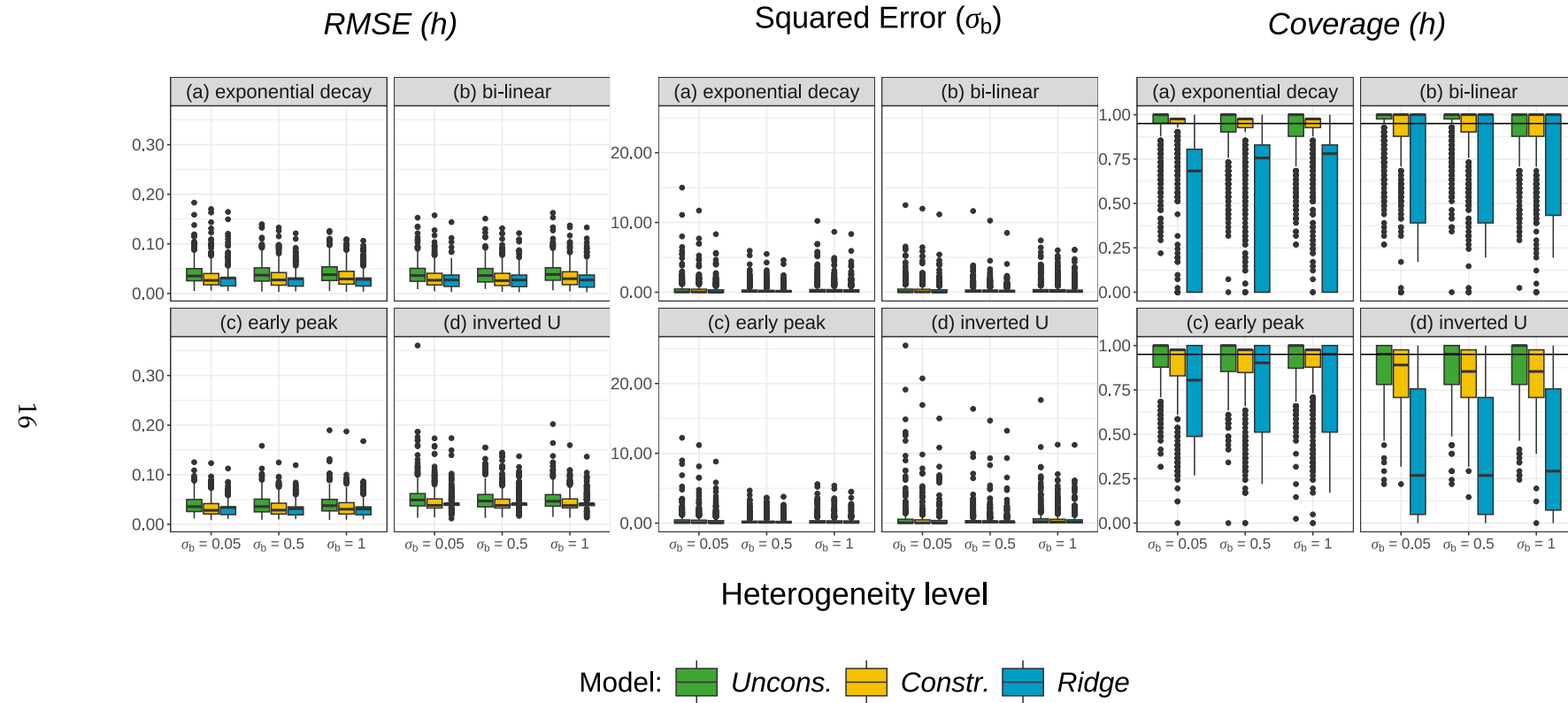


Figure S5: Distribution of the RMSE of $h(t, t_z, z(t_z))$, 95% point-wise Coverage of $h(t, t_z, z(t_z))$ and the squared error of σ_b for $L = 20$ players and across all other simulation settings ($N_{\text{sim}} = 500$).

L = 40 players

17

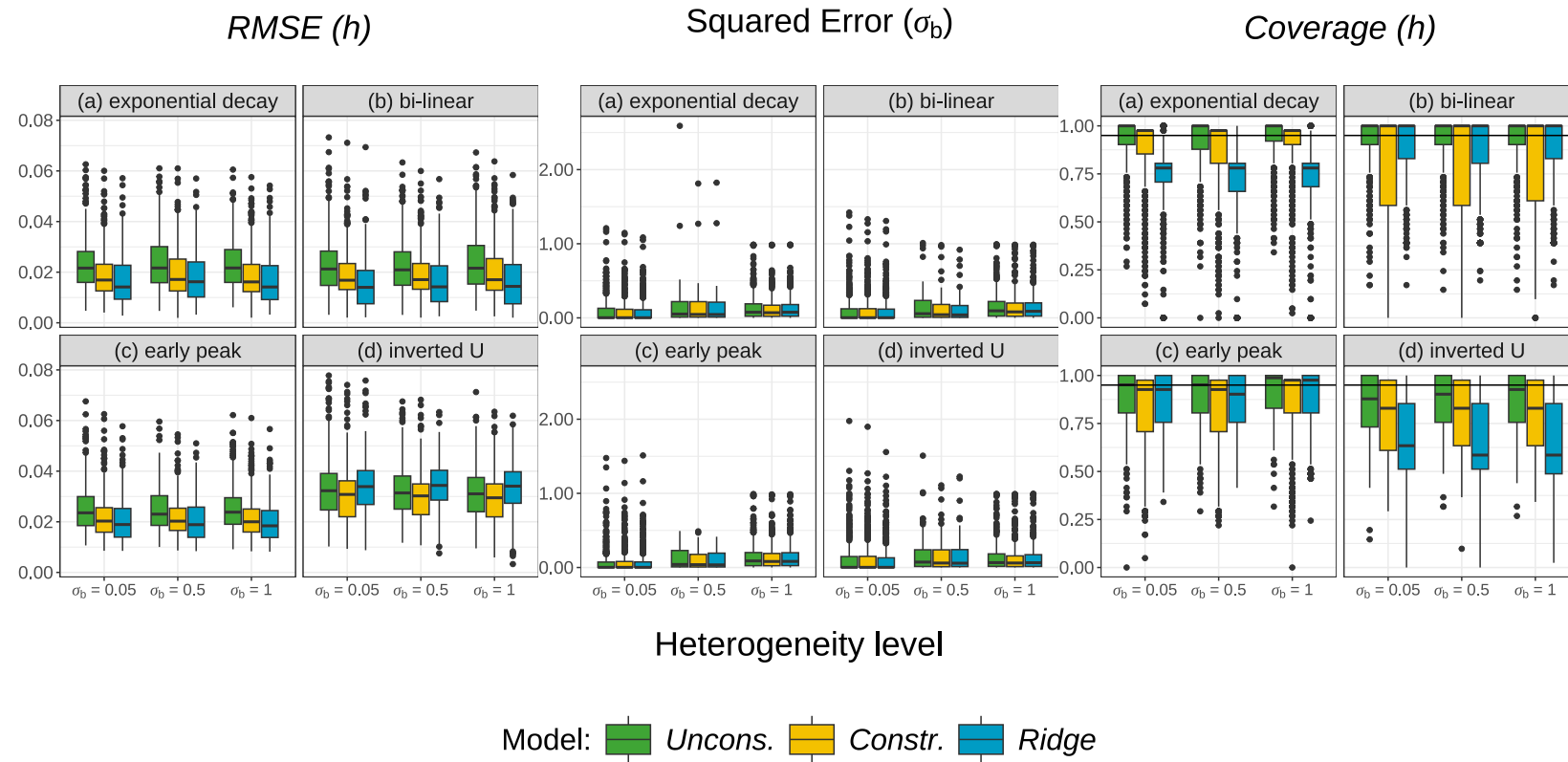


Figure S6: Distribution of the RMSE of $h(t, t_z, z(t_z))$, 95% point-wise Coverage of $h(t, t_z, z(t_z))$ and the squared error of σ_b for $L = 40$ players and across all other simulation settings ($N_{\text{sim}} = 500$).

$L = 100$ players

18

RMSE (h)

Squared Error (σ_b)

Coverage (h)

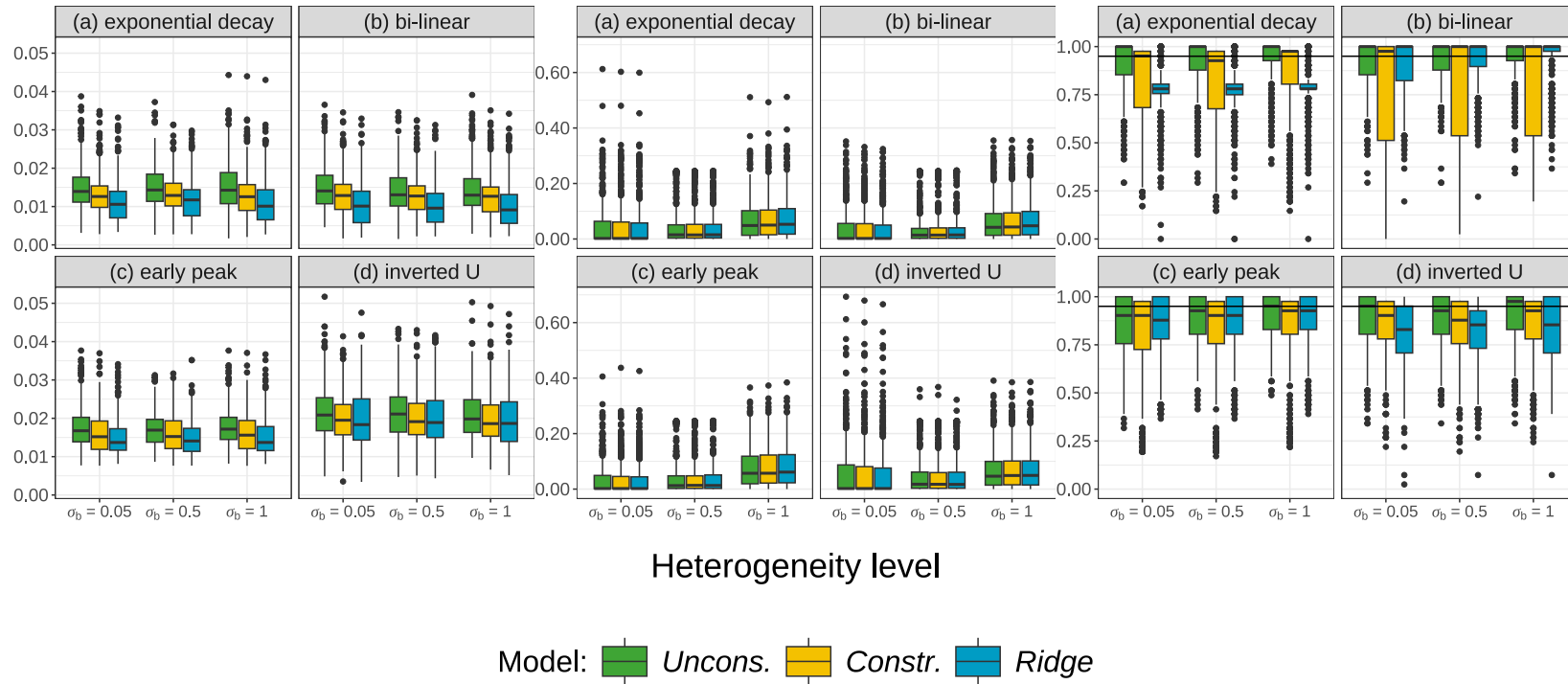


Figure S7: Distribution of the RMSE of $h(t, t_z, z(t_z))$, 95% point-wise Coverage of $h(t, t_z, z(t_z))$ and the squared error of σ_b for $L = 100$ players and across all other simulation settings ($N_{\text{sim}} = 500$).

L = 20 players

(a) exponential decay

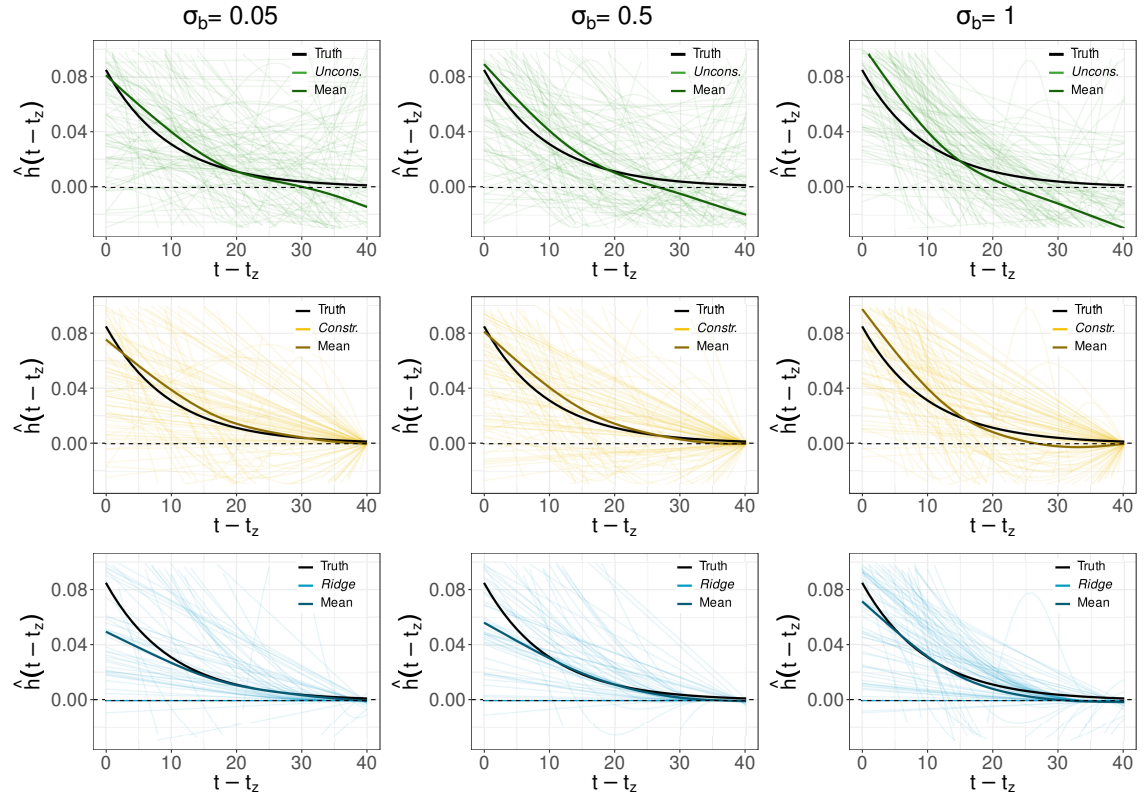


Figure S8: A random sample of 100 estimated weight functions for the *Uncons.* model (1st row, light green), *Constr.* (2nd row, light yellow) and *Ridge* model (3rd row, light blue), for $L = 20$ players and for scenarios $\sigma_b = 0.05$ (left), $\sigma_b = 0.5$ (middle) and $\sigma_b = 1$ (right), together with the true weight function (in black), shape (a), and the mean curve (in darker color corresponding to the model).

L = 40 players

(a) exponential decay

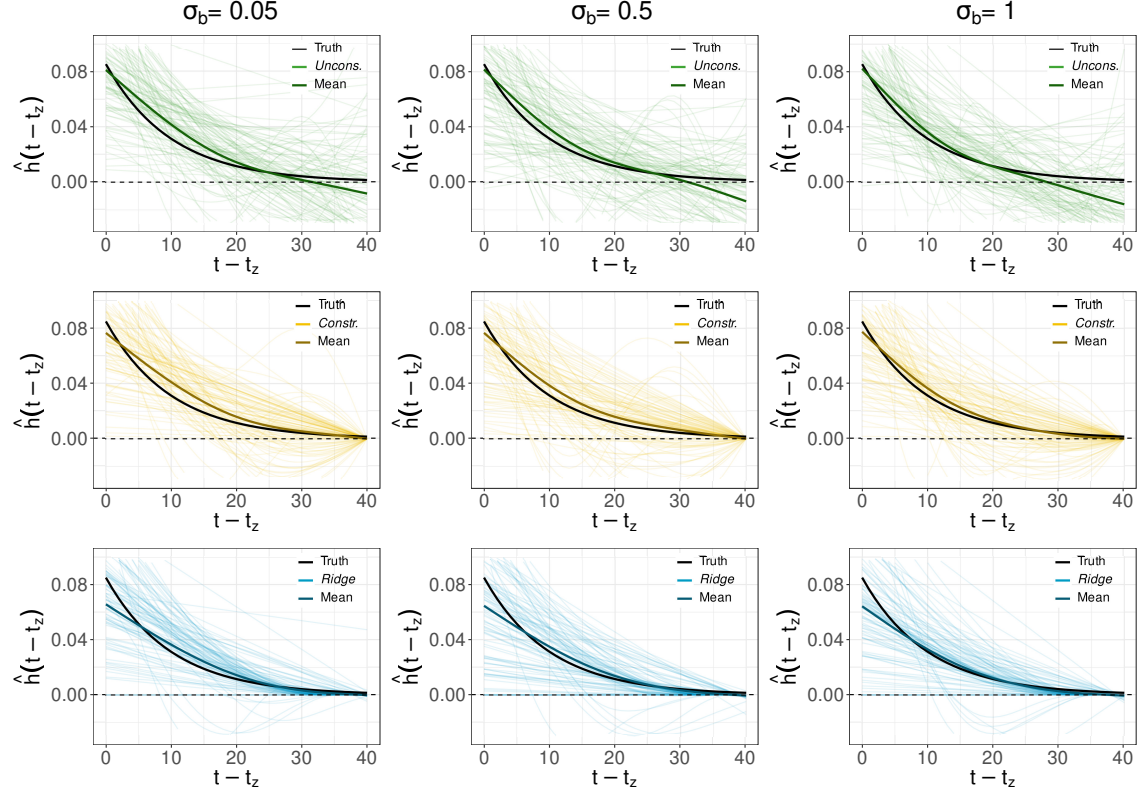


Figure S9: A random sample of 100 estimated weight functions for the *Uncons.* model (1st row, light green), *Constr.* (2nd row, light yellow) and *Ridge* model (3rd row, light blue), for $L = 40$ players and for scenarios $\sigma_b = 0.05$ (left), $\sigma_b = 0.5$ (middle) and $\sigma_b = 1$ (right), together with the true weight function (in black), shape (a), and the mean curve (in darker color corresponding to the model).

$L = 100$ players

(a) exponential decay

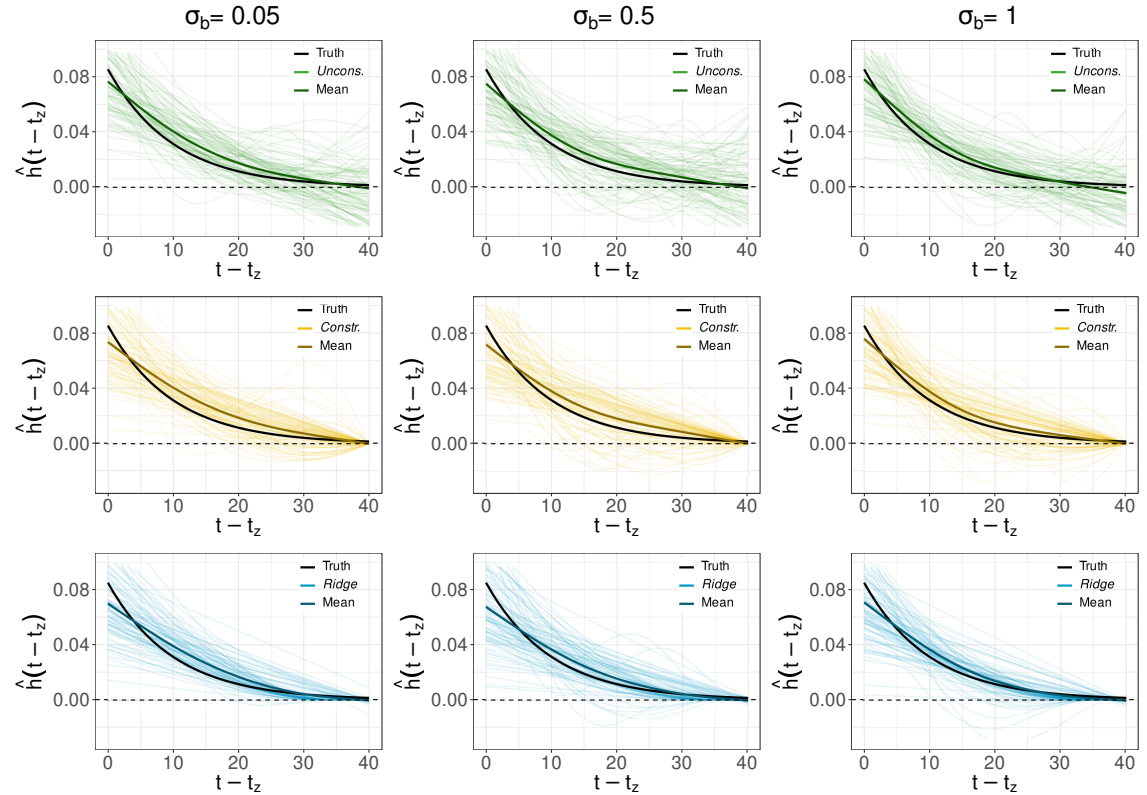


Figure S10: A random sample of 100 estimated weight functions for the *Uncons.* model (1st row, light green), *Constr.* (2nd row, light yellow) and *Ridge* model (3rd row, light blue), for $L = 100$ players and for scenarios $\sigma_b = 0.05$ (left), $\sigma_b = 0.5$ (middle) and $\sigma_b = 1$ (right), together with the true weight function (in black), shape (a), and the mean curve (in darker color corresponding to the model).

L = 20 players

(b) bi-linear

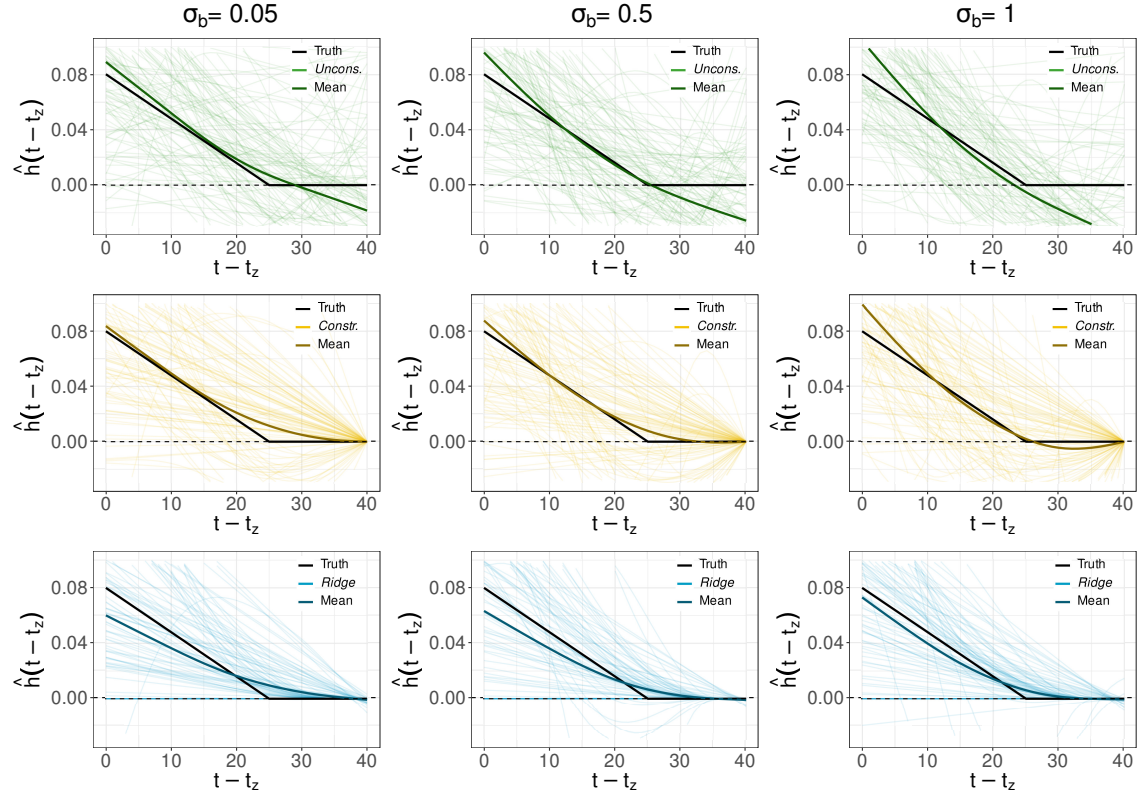


Figure S11: A random sample of 100 estimated weight functions for the *Uncons.* model (1st row, light green), *Constr.* (2nd row, light yellow) and *Ridge* model (3rd row, light blue), for $L = 20$ players and for scenarios $\sigma_b = 0.05$ (left), $\sigma_b = 0.5$ (middle) and $\sigma_b = 1$ (right), together with the true weight function (in black), shape (b), and the mean curve (in darker color corresponding to the model).

L = 40 players

(b) bi-linear

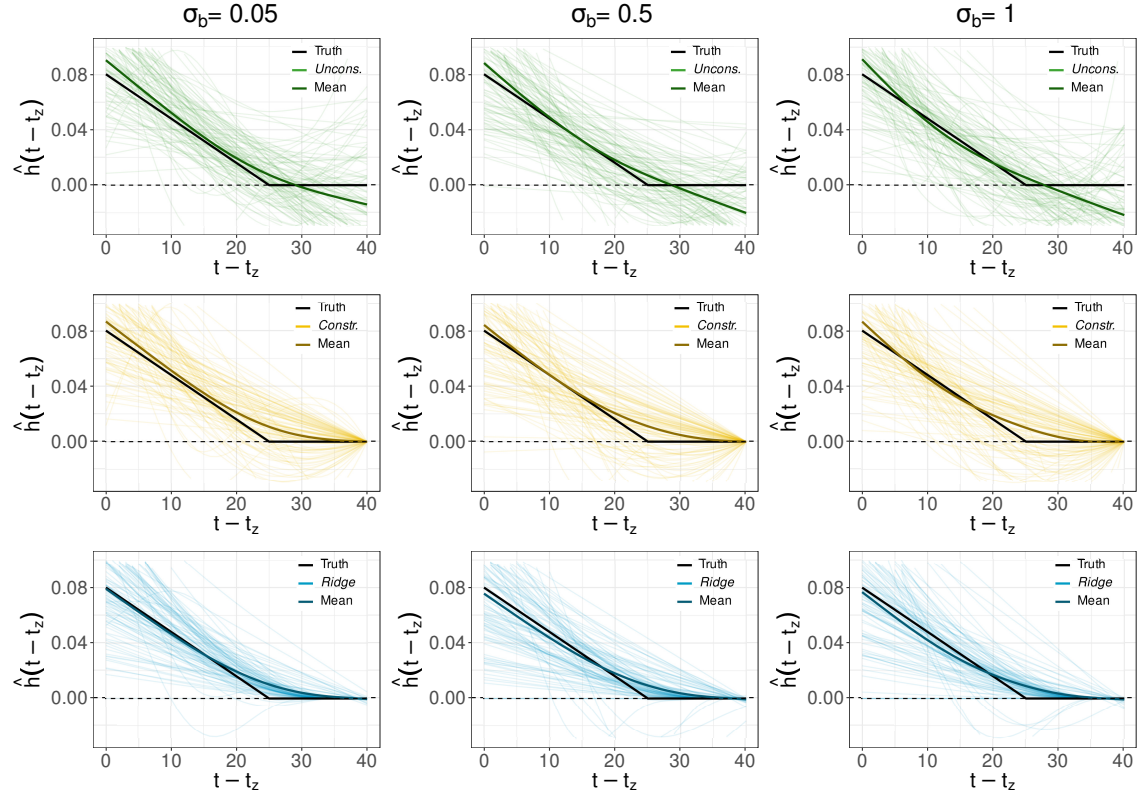


Figure S12: A random sample of 100 estimated weight functions for the *Uncons.* model (1st row, light green), *Constr.* (2nd row, light yellow) and *Ridge* model (3rd row, light blue), for $L = 40$ players and for scenarios $\sigma_b = 0.05$ (left), $\sigma_b = 0.5$ (middle) and $\sigma_b = 1$ (right), together with the true weight function (in black), shape (b), and the mean curve (in darker color corresponding to the model).

$L = 100$ players

(b) bi-linear

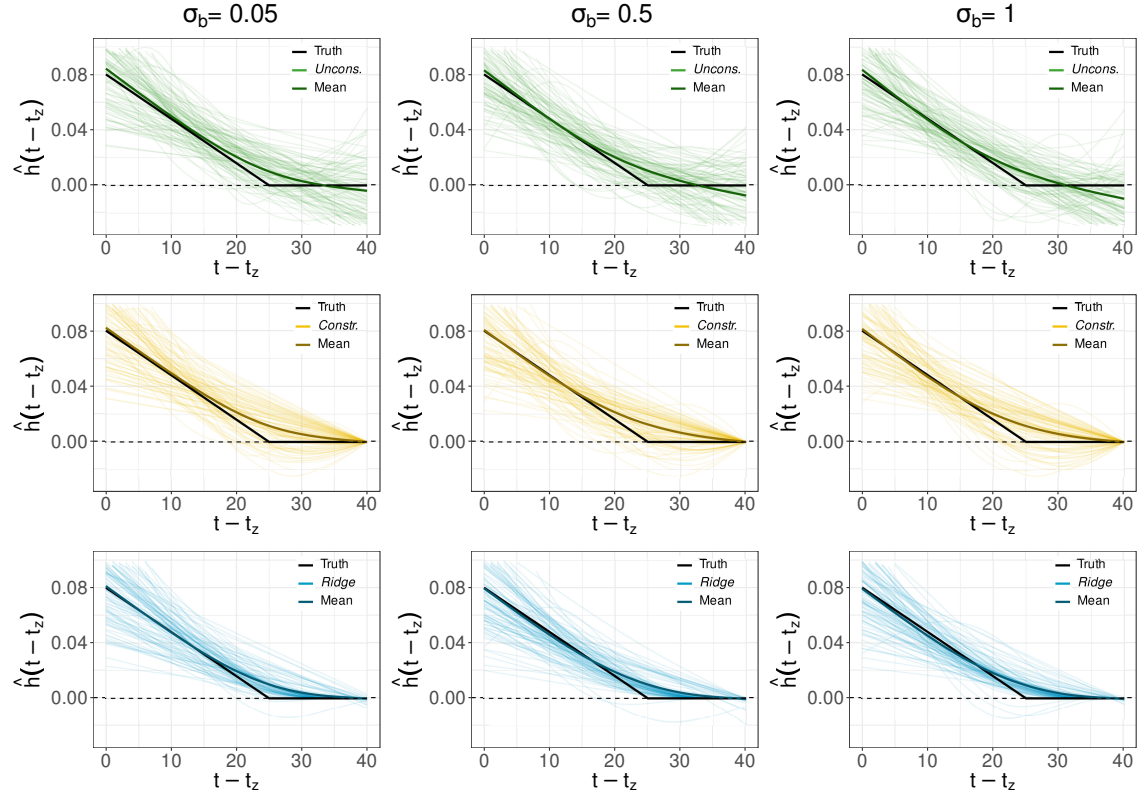


Figure S13: A random sample of 100 estimated weight functions for the *Uncons.* model (1st row, light green), *Constr.* (2nd row, light yellow) and *Ridge* model (3rd row, light blue), for $L = 100$ players and for scenarios $\sigma_b = 0.05$ (left), $\sigma_b = 0.5$ (middle) and $\sigma_b = 1$ (right), together with the true weight function (in black), shape (b), and the mean curve (in darker color corresponding to the model).

L = 20 players

(c) early peak

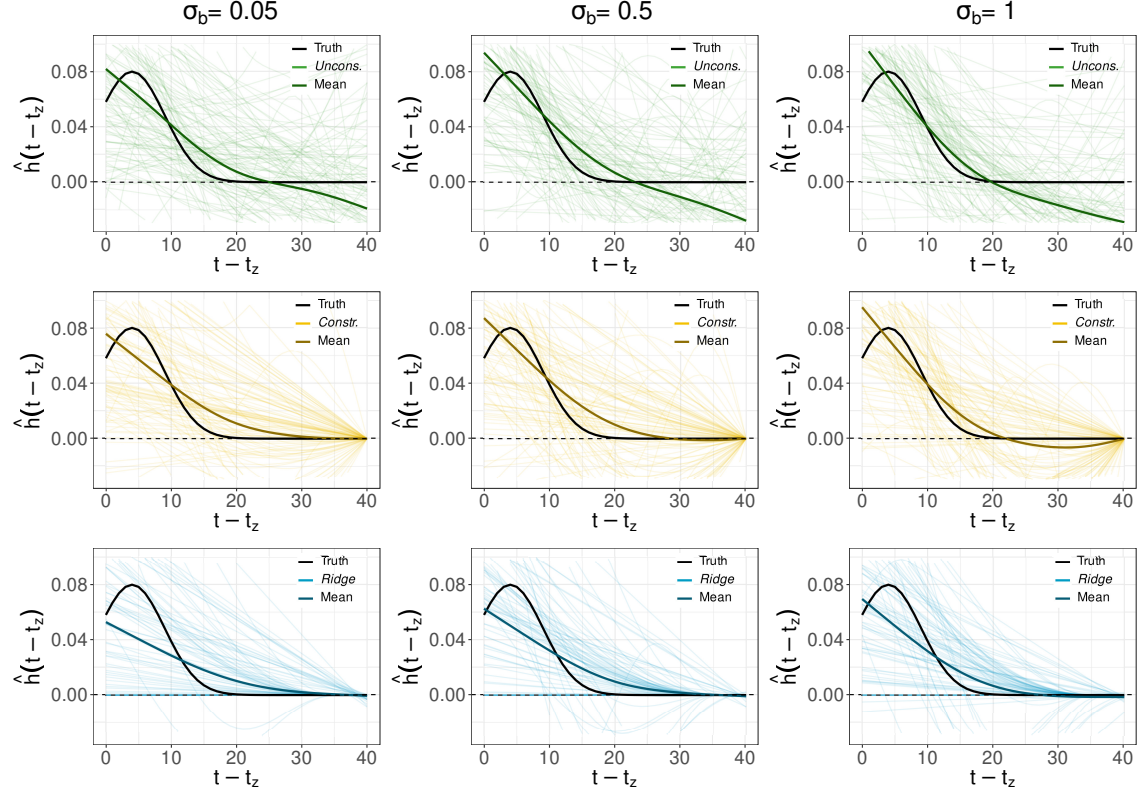


Figure S14: A random sample of 100 estimated weight functions for the *Uncons.* model (1st row, light green), *Constr.* (2nd row, light yellow) and *Ridge* model (3rd row, light blue), for $L = 20$ players and for scenarios $\sigma_b = 0.05$ (left), $\sigma_b = 0.5$ (middle) and $\sigma_b = 1$ (right), together with the true weight function (in black), shape (c), and the mean curve (in darker color corresponding to the model).

L = 40 players

(c) early peak

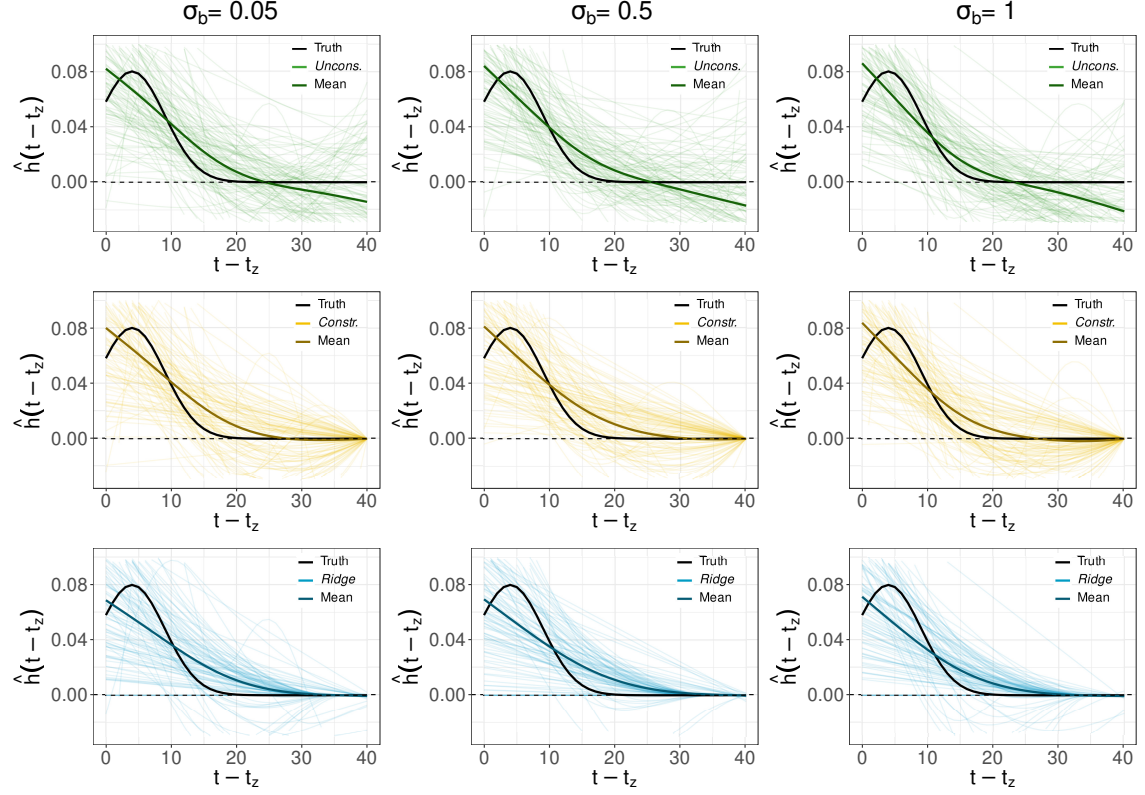


Figure S15: A random sample of 100 estimated weight functions for the *Uncons.* model (1st row, light green), *Constr.* (2nd row, light yellow) and *Ridge* model (3rd row, light blue), for $L = 40$ players and for scenarios $\sigma_b = 0.05$ (left), $\sigma_b = 0.5$ (middle) and $\sigma_b = 1$ (right), together with the true weight function (in black), shape (c), and the mean curve (in darker color corresponding to the model).

L = 100 players

(c) early peak

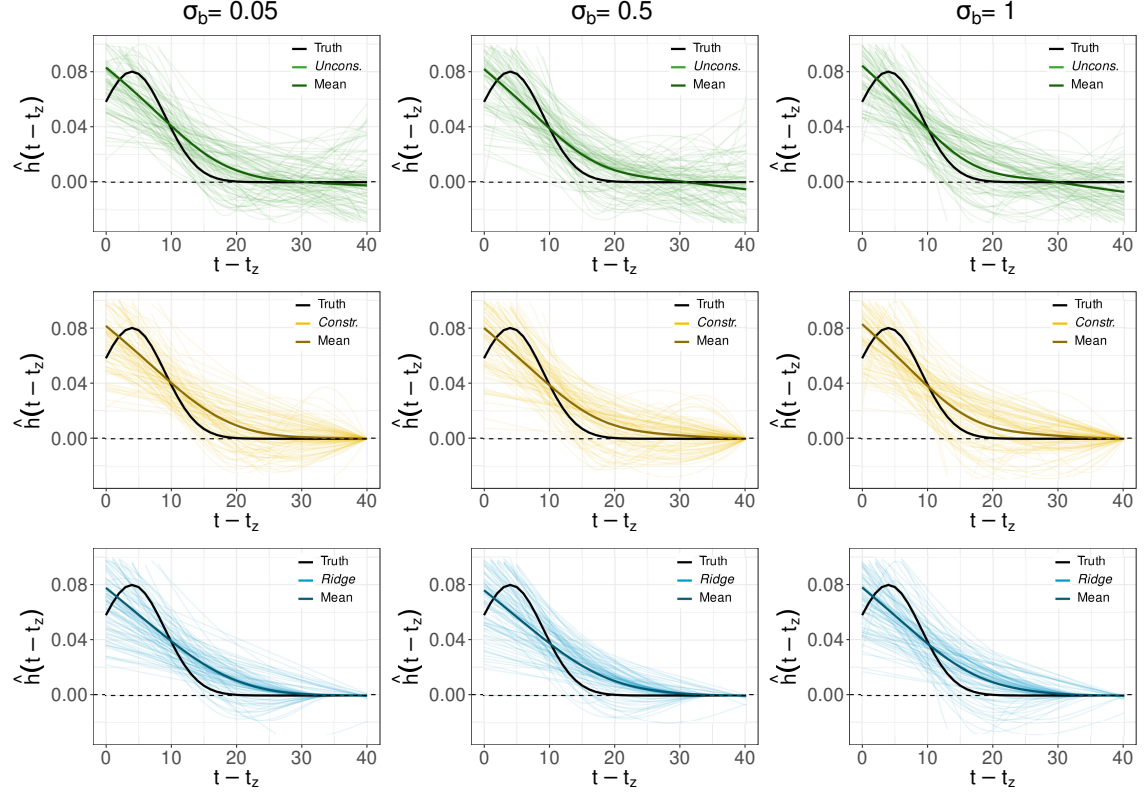


Figure S16: A random sample of 100 estimated weight functions for the *Uncons.* model (1st row, light green), *Constr.* (2nd row, light yellow) and *Ridge* model (3rd row, light blue), for $L = 100$ players and for scenarios $\sigma_b = 0.05$ (left), $\sigma_b = 0.5$ (middle) and $\sigma_b = 1$ (right), together with the true weight function (in black), shape (c), and the mean curve (in darker color corresponding to the model).

L = 20 players

(d) inverted U

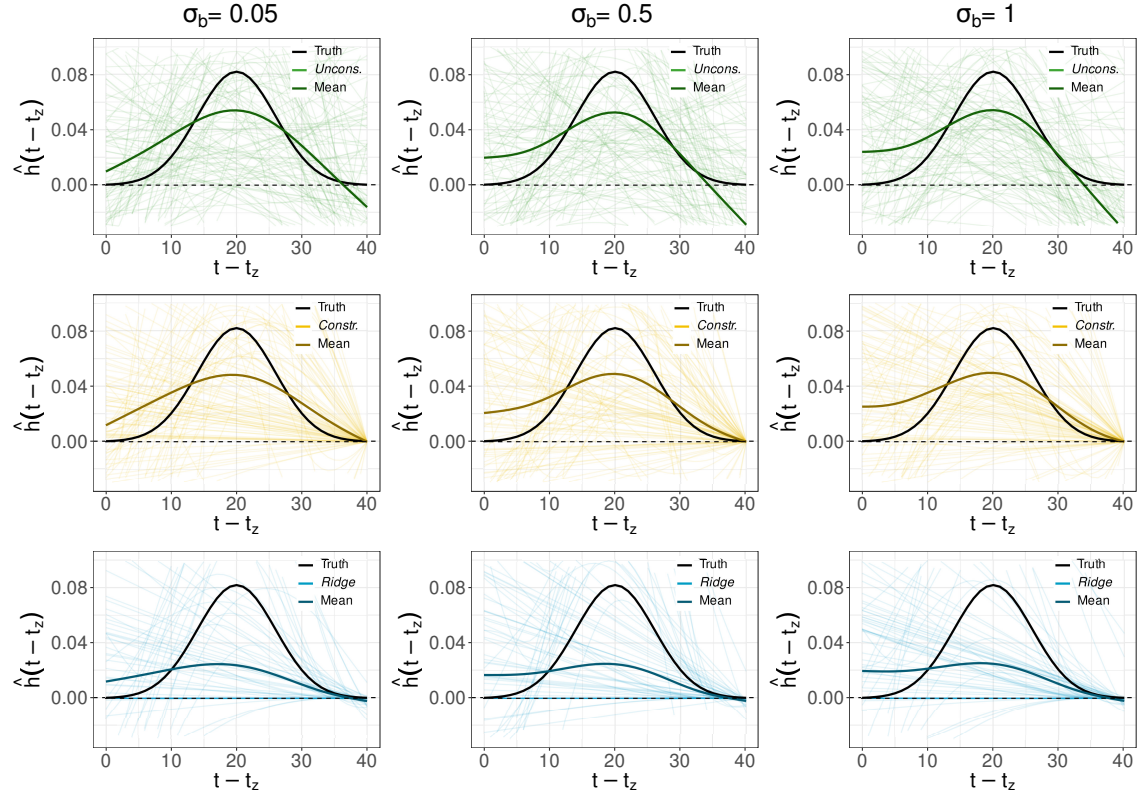


Figure S17: A random sample of 100 estimated weight functions for the *Uncons.* model (1st row, light green), *Constr.* (2nd row, light yellow) and *Ridge* model (3rd row, light blue), for $L = 20$ players and for scenarios $\sigma_b = 0.05$ (left), $\sigma_b = 0.5$ (middle) and $\sigma_b = 1$ (right), together with the true weight function (in black), shape (d), and the mean curve (in darker color corresponding to the model).

L = 40 players

(d) inverted U

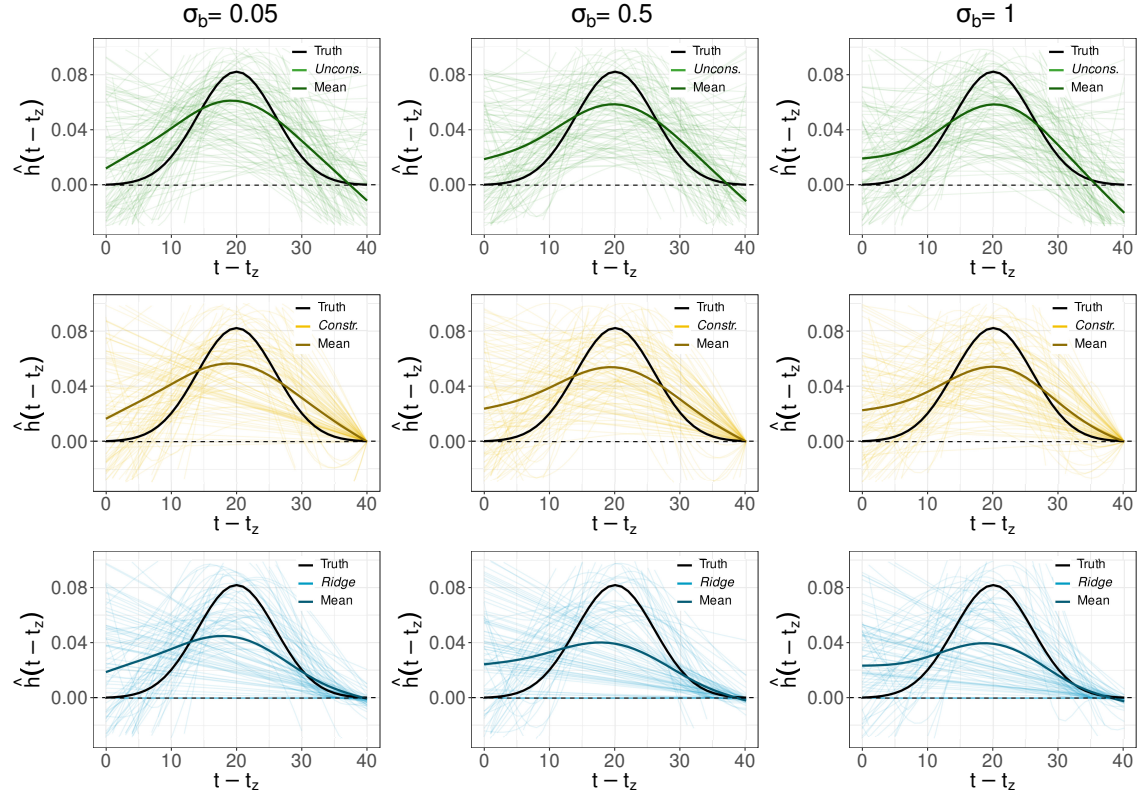


Figure S18: A random sample of 100 estimated weight functions for the *Uncons.* model (1st row, light green), *Constr.* (2nd row, light yellow) and *Ridge* model (3rd row, light blue), for $L = 40$ players and for scenarios $\sigma_b = 0.05$ (left), $\sigma_b = 0.5$ (middle) and $\sigma_b = 1$ (right), together with the true weight function (in black), shape (d), and the mean curve (in darker color corresponding to the model).

L = 100 players

(d) inverted U

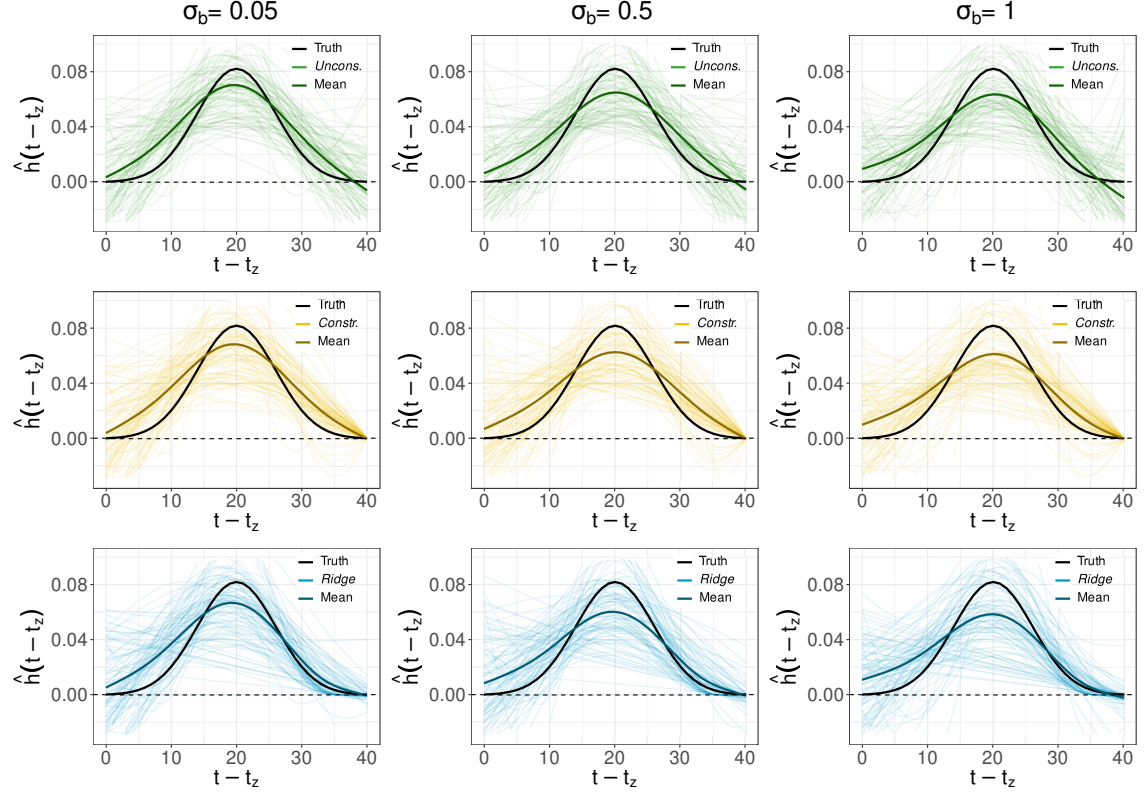


Figure S19: A random sample of 100 estimated weight functions for the *Uncons.* model (1st row, light green), *Constr.* (2nd row, light yellow) and *Ridge* model (3rd row, light blue), for $L = 100$ players and for scenarios $\sigma_b = 0.05$ (left), $\sigma_b = 0.5$ (middle) and $\sigma_b = 1$ (right), together with the true weight function (in black), shape (a), and the mean curve (in darker color corresponding to the model).

Table S8: Frequency of the models that yield best BIC and Deviance explained in each replication of the simulation, $N_{\text{sim}} = 500$, across all scenarios.

		Data generation mechanism								
L players	WCE shape	Heterogeneity	Lowest	Lowest	Lowest	Largest	Largest	Largest		
			BIC	BIC	BIC	Dev.	Dev.	Dev.		
			<i>Uncons.</i>	<i>Constr.</i>	<i>Ridge</i>	<i>Uncons.</i>	<i>Constr.</i>	<i>Ridge</i>		
L = 20 players	(a) Exponential decay	$\sigma_b = 0.05$	3	18	79	74	21	5		
		$\sigma_b = 0.5$	7	21	72	70	25	5		
		$\sigma_b = 1$	7	29	64	72	22	5		
	(b) Bi-linear	$\sigma_b = 0.05$	4	22	74	74	18	8		
		$\sigma_b = 0.5$	9	22	68	65	27	8		
		$\sigma_b = 1$	12	30	58	67	27	6		
	(c) Early peak	$\sigma_b = 0.05$	5	15	80	75	19	6		
		$\sigma_b = 0.5$	10	21	69	68	26	6		
		$\sigma_b = 1$	11	27	62	68	26	6		
	(d) Inverted U	$\sigma_b = 0.05$	3	13	84	83	13	4		
		$\sigma_b = 0.5$	6	17	77	81	14	5		
		$\sigma_b = 1$	6	21	73	81	16	3		

Table S9: Frequency of the models that yield best BIC and Deviance explained in each replication of the simulation, $N_{\text{sim}} = 500$, across all scenarios (continuation).

Data generation mechanism								
L players	WCE shape	Heterogeneity	Lowest	Lowest	Lowest	Largest	Largest	Largest
			BIC	BIC	BIC	Dev.	Dev.	Dev.
			<i>Uncons.</i>	<i>Constr.</i>	<i>Ridge</i>	<i>Uncons.</i>	<i>Constr.</i>	<i>Ridge</i>
			(%)	(%)	(%)	(%)	(%)	(%)
L = 40 players	(a) Exponential decay	$\sigma_b = 0.05$	6	25	68	69	22	8
		$\sigma_b = 0.5$	10	28	62	63	27	10
		$\sigma_b = 1$	14	29	57	57	36	7
	(b) Bi-linear	$\sigma_b = 0.05$	11	28	61	66	26	9
		$\sigma_b = 0.5$	17	27	56	56	35	9
		$\sigma_b = 1$	17	29	53	52	39	9
	(c) Early peak	$\sigma_b = 0.05$	9	22	69	65	25	9
		$\sigma_b = 0.5$	15	23	63	64	29	7
		$\sigma_b = 1$	15	27	57	54	37	9
	(d) Inverted U	$\sigma_b = 0.05$	6	30	64	79	15	6
		$\sigma_b = 0.5$	8	31	60	78	15	7
		$\sigma_b = 1$	9	34	56	68	25	7

Table S10: Frequency of the models that yield best BIC and Deviance explained in each replication of the simulation, $N_{\text{sim}} = 500$, across all scenarios (continuation).

Data generation mechanism								
L players	WCE shape	Heterogeneity	Lowest	Lowest	Lowest	Largest	Largest	Largest
			BIC	BIC	BIC	Dev.	Dev.	Dev.
			<i>Uncons.</i>	<i>Constr.</i>	<i>Ridge</i>	<i>Uncons.</i>	<i>Constr.</i>	<i>Ridge</i>
			(%)	(%)	(%)	(%)	(%)	(%)
L = 100 players	(a) Exponential decay	$\sigma_b = 0.05$	3	30	67	77	12	11
		$\sigma_b = 0.5$	3	37	60	85	10	5
		$\sigma_b = 1$	2	31	67	86	10	4
	(b) Bi-linear	$\sigma_b = 0.05$	3	29	67	68	19	12
		$\sigma_b = 0.5$	5	27	69	79	16	5
		$\sigma_b = 1$	5	26	68	74	22	3
	(c) Early peak	$\sigma_b = 0.05$	3	17	79	76	15	9
		$\sigma_b = 0.5$	3	15	83	85	12	3
		$\sigma_b = 1$	3	16	81	81	15	4
	(d) Inverted U	$\sigma_b = 0.05$	3	35	62	67	14	19
		$\sigma_b = 0.5$	5	44	52	75	14	11
		$\sigma_b = 1$	5	47	48	81	12	8

References

- Bender A, Scheipl F, Hartl W, et al. Penalized estimation of complex, non-linear exposure-lag-response associations. *Biostatistics* 2019; 20(2): 315–331.
- Sylvestre MP, Abrahamowicz M. Flexible modeling of the cumulative effects of time-dependent exposures on the hazard. *Stat Med* 2009; 28(27): 3437–3453.
- Killen NM, Gabbett TJ and Jenkins DG. Training loads and incidence of injury during the preseason in professional rugby league players. *The Journal of Strength & Conditioning Research* 2010; 24(8): 2079–2084.
- Gabbett TJ, Hulin BT, Blanch P et al. High training workloads alone do not cause sports injuries: how you get there is the real issue. *British journal of sports medicine* 2016; 50(8): 444–445.
- Banister EW and Calvert TW. Planning for future performance: implications for long term training. Canadian journal of applied sport sciences. *Journal canadien des sciences appliquées au sport* 1980; 5(3): 170–176.
- Wang C, Vargas JT, Stokes T et al. Analyzing activity and injury: lessons learned from the acute: chronic workload ratio. *Sports Medicine* 2020; 50(7); 1243–1254.